

# Neutron Multiple Diffraction in Structural Analysis

C.B.R. Parente and V.L. Mazzocchi

*Instituto de Pesquisas Energéticas e Nucleares  
Comissão Nacional de Energia Nuclear  
CP 11049 - Pinheiros - 05422-970 - São Paulo, SP, Brazil*

---

## Abstract

Neutron multiple diffraction (n.m.d.) has been recently developed as a method for analysis of crystal and magnetic structures. To apply the method, a computer program (MULTI) has been written in order to simulate n.m.d. patterns in cases of high density of simultaneous reflections and high secondary extinction. In a first application of the method,  $\alpha$ - and  $\beta$ -quartz structures of silica ( $\text{SiO}_2$ ) have been analysed.  $\alpha$ -quartz has a structure described by either of the two enantiomorphic trigonal space groups  $P3_121$  or  $P3_221$ . At ca. 846K,  $\alpha$ -quartz undergoes a reversible transition to  $\beta$ -quartz.  $\beta$ -quartz has a structure with hexagonal symmetry in either of the two enantiomorphic space groups  $P6_222$  or  $P6_422$ . 'Umweganregung' n.m.d. patterns were obtained by measuring the 001 space-group-forbidden primary reflection, at room temperature for the  $\alpha$  phase and ca. 1003K for the  $\beta$  phase. Simulated patterns were calculated for both phases by assuming structures previously reported in the literature. Agreement between experimental and simulated patterns was verified by calculating a reliability factor R, where experimental and calculated integrated intensities of peaks are compared. For a well-known ordered model of the  $\alpha$ -quartz structure, R resulted equal to 0.344. For  $\beta$ -quartz, an ordered and a disordered model of structure were both analysed. In the disordered model, oxygen atoms occupy, in a half-occupation mode, twice the number of special positions they occupy in the ordered model. A better R figure was found for the disordered model, when compared to that found for the ordered one, namely  $R = 0.110$  and  $R = 0.143$ , respectively. No refinement of parameters was attempted in this study. In a second application of the method, structural parameters for both ferrimagnetic and paramagnetic phases of magnetite have been refined from n.m.d. data. At room temperature, magnetite is an inversed iron spinel with a Néel A-B magnetic structure in the cubic space group  $Fm\bar{3}m$ . Above ca. 853K, the magnetic order in magnetite vanishes and it becomes a paramagnet. 'Aufhellung' n.m.d. patterns were obtained by measuring the 111 primary reflection of magnetite, at room temperature for the ferrimagnetic phase and ca. 976K for the paramagnetic phase. Agreement was verified in a point-to-point basis by a profile R factor where observed and calculated intensities, for each azimuthal position, are compared. Thermal parameters were considered in the refinements in three different ways: i) an overall isotropic parameter for all ions in the structure; ii) different isotropic parameters, one for each special position occupied by ions in the structure; iii) anisotropic parameters for all ions in the structure. For both phases, best results were found in those refinements done according iii) above. In this case, profile R factors resulted equal to 0.030 and 0.033 for ferrimagnetic and paramagnetic phases, respectively. Refined parameters for the ferrimagnetic phase were compared to results of refinements reported in the literature. Such a comparison showed the consistency of the n.m.d. as a method for structural analysis. No results were found in the literature for the paramagnetic phase.

---

## 1. Introduction

Diffraction, as commonly known, is a particular phenomenon of a more general one: multiple diffraction. Multiple diffraction occurs when a single crystal is positioned to diffract a neutron or X-ray incident beam, by a family of crystallographic planes, and, simultaneously, other families are also in position to diffract the same beam (Chang, 1984). Occurrence of the general phenomenon is by no means uncommon. It may even be unavoidable, at all. This is particularly the case when working at short wavelengths or with crystals of large cell dimensions (Arndt and Willis, 1966). An extreme situation occurs when both conditions above coexist. In single-crystal (single) X-ray and neutron diffractometry, multiple

diffraction can be considered as a disturbance, causing errors in measured intensities or an apparent violation of the systematic extinctions. In the former case above, it is very difficult to identify the effect unless the crystal is turned around the scattering vector of the reflection being measured in order to look for variations in the intensity of the reflection. In the latter case, peaks have a different shape than that of normal peaks, turning them easily recognizable (Giacovazzo, 1991).

The occurrence of simultaneous reflections, in the manner described above, is totally casual. It was Renninger (1937), in a study of the X-ray multiple diffraction phenomenon in diamond and rock salt, who found the way to produce the systematic

appearance of multiple diffraction peaks. He found that, turning the crystal around the scattering vector of a reflection a variation in the intensity is observed. Renninger obtained both 'Umweganregung' ('Umweg') and 'Aufhellung' patterns in his study. This procedure became known as Renninger scan or  $\phi$ -scan. It has been used (since then) by several authors to obtain multiple diffraction patterns (of X-rays or neutrons) for different studies. For many years, works dealing with the modification of shape and intensity of a peak, obtained in a (single) neutron diffraction measurement, by effect of multiple diffraction (Borgonovi and Cagliotti, 1962), indexing of multiple diffraction patterns (Cole, Chambers and Dunn, 1962), calculation of intensities in neutron multiple diffraction (Moon and Shull, 1964) and application of X-ray multiple diffraction to determine the mosaic spread of a crystal (Caticha-Ellis, 1969) and to solve the phase problem in crystal structure determination (Post, 1977 and 1979; Chang, 1981 and 1982) have been published sporadically in the literature. Although still scarce, publication of works about multiple diffraction became more frequent in recent years.

In 1984, Mazzocchi studied the  $\alpha$  and  $\beta$  phases of quartz by using neutron multiple diffraction (n.m.d.) as a method for structural analysis. As far as we know, this was the first time the general phenomenon of diffraction was used in structural analysis. The analyses of both phases of quartz were performed by using a computer program, MULTI, written to simulate n.m.d. patterns (Mazzocchi and Parente, 1994). MULTI uses approximate intensity solutions derived for a many-beam case. These solutions are based in the iterative method (Parente and Caticha-Ellis, 1974a; Chang, 1984) for the calculation of intensities. This method is an extension to high absorption and high secondary extinction cases of the theory developed by Moon and Shull (1964) for the multiple diffraction of neutrons in a mosaic crystal. Moon and Shull calculated the intensity of a particular beam by summing the terms of a Taylor series expansion of the powers of the different beams participating in the phenomenon. They presented analytical formulas retaining terms up to the third order. A low order limitates the calculation of intensities to cases of low absorption and low secondary extinction. These cases are, in general, feasible if thin crystals are used. Thin crystals plus neutron diffraction, on the other hand, is not a good combination since diffracted intensities become very weak owing to a small diffracting volume. To cope with this problem, Parente and Caticha-Ellis (1974a) derived the general term for the Taylor series expansion. With the general term and a computer, it became possible to calculate intensities in an iterative way till any desired order.

In what follows, a brief description of the experimental arrangement, theory and computer

program MULTI, used in the analyses by the n.m.d. method, are presented. Results obtained by applying the n.m.d. method in the above mentioned study of  $\alpha$ - and  $\beta$ -quartz (Mazzocchi, 1984; Mazzocchi and Parente, 1994, for  $\beta$ -quartz alone), as well as recent results for the refinement of structural parameters of the ferrimagnetic and paramagnetic phases of magnetite are also presented.

## 2. Experimental Arrangement

To obtain n.m.d. patterns, an experimental arrangement is assembled in the IPEN neutron diffractometer installed at the IEA-R1 2 MW research reactor. This arrangement includes, besides the normal parts of a neutron diffractometer, a special collimator for n.m.d. experiments and a five-circle goniometer. Optionally, an extra detector may be installed aligned with the incident beam. This detector allows for the measurement of transmitted beam n.m.d. patterns.

Figure 1 is a scheme of the arrangement showing the special m.d. collimator, the extra detector and the detector ( $BF_3$ ) normally used in the neutron diffractometer. Figure 1 also gives an idea of the geometry of the experiment. The four kinds of pattern that can be observed in a m.d. experiment (Mazzocchi and Parente, 1994) are shown in the Figure. Depending on the intensity of the primary reflection, null, weak or strong, patterns can be type 'Umweg', mixed 'Aufhellung/Umweg' or 'Aufhellung', respectively. The transmitted beam pattern is always 'Aufhellung' type.

The special collimator limits the angular divergence of the monochromatic beam in both vertical and horizontal directions to a few minutes of arc (Mazzocchi, 1984). It is, actually, an evolution of the collimator conceived by Parente and Caticha-Ellis (1974b) to be used in n.m.d. experiments in order to obtain patterns with good resolution.

The IPEN neutron diffractometer is normally equipped with a five-circle goniometer. This goniometer has, in addition to the axes  $\theta$ ,  $\omega$ ,  $\phi$ , and  $\chi$  of a four-circle goniometer, an extra  $\Sigma$ -axis which can be set along the scattering vector of a primary reflection (Parente and Caticha-Ellis, 1974b).

For high temperature measurements, an electrical furnace was designed and constructed (Mazzocchi, 1984; Mazzocchi and Parente, 1994). A simplified drawing of this furnace is shown in Figure 2.

## 3. Theory Used in the Intensity Calculations

In 1964, Moon and Shull presented a theory for the multiple diffraction of neutrons in a mosaic crystal having the shape of a flat plate large compared with the incident beam cross section.

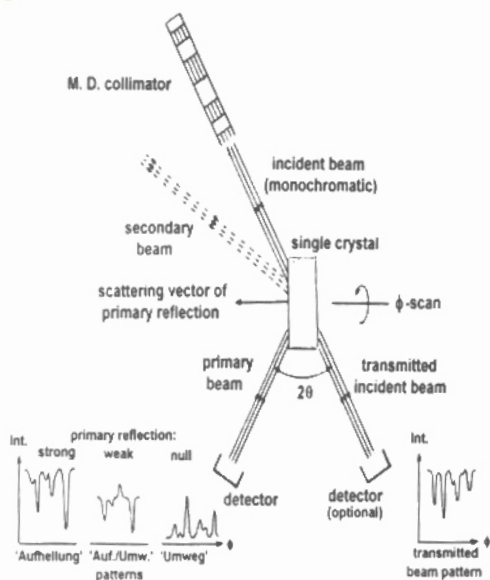


Fig. 1 Experimental arrangement used in n.m.d. experiments.

This theory is an extension of the kinematical treatment of the secondary extinction developed for the (single) neutron diffraction in mosaic crystals (see, for example, Bacon and Lowde, 1948). Primary extinction is assumed to be negligible.

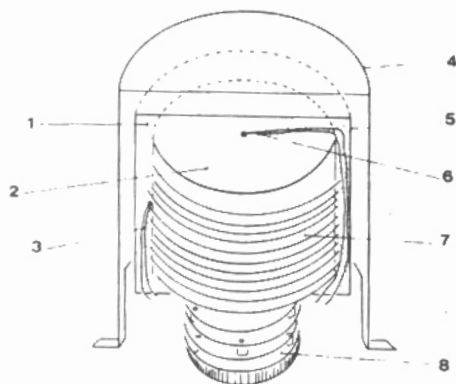


Fig. 2 Schematic view of the furnace employed in high temperature measurements. Numbers indicate: 1. sustaining powder; 2. sample; 3. thermocouple (for temperature control); 4. heat shield; 5. stainless steel capsule; 6. thermocouple (to indicate sample temperature); 7. heating resistance; 8. thermal insulator.

Moon and Shull's differential equations, describing the change in power in the several beams traversing a layer of thickness  $dx$  at depth  $x$  below the surface of a crystal plate, can be written in the following concise form (Parente and Caticha-Ellis, 1974 a):

$$P_i^{(1)}(x) = s_i \sum_{j \neq i} \left[ P_j(x) / \gamma_j \right] \bar{Q}_{ji} - s_i P_i(x) (A_i / \gamma_i)$$

where  $P_i^{(1)}(x) = dP_i(x) / dx$

and  $s_i = +1$ , if beam  $i$  is transmitted, or  $s_i = -1$ , if reflected.

Coefficients  $A_i$  are given by

$$A_i = \mu + \sum_{j \neq i} \bar{Q}_{ij}$$

Symbols  $P_i, P_j, s_i, \mu, \bar{Q}_{ij}$  and  $\gamma_i$  are, respectively, the power in beam  $i$ , the power in a beam  $j \neq i$ , the sign of beam  $i$  characterizing its type (as above), the linear absorption coefficient, the linear reflection coefficient (or simply reflectivity) for the exchange of power from beam  $i$  to beam  $j$  and the magnitude of the direction cosine of the beam  $i$  relative to the normal to the crystal surface. Subscripts  $i$  and  $j$  refer to all beams involved in the phenomenon including incident and primary beams.

According to Moon and Shull (1964) the reflectivity for an interaction  $i \rightarrow j$  is given by

$$r_{ij} = Q_{ij} W(\Delta\theta_{ij}),$$

where  $Q_{ij}$  is the integrated reflectivity per unit volume of a small crystallite and  $W(\Delta\theta_{ij})$  is the mosaic distribution function where  $\Delta\theta_{ij}$  is the deviation in the Bragg angle  $\theta_{ij}$  from the mean of the distribution.

Moon and Shull (1964) proposed a Taylor series expansion of  $P_i(x)$  about the point  $x=0$ , as a useful approximate solution for the intensity of the primary beam. They derived an analytical formula for the expansion retaining terms up to the second order. As pointed out in the work, the formula is valid only in the limits of low secondary extinction and low absorption. Caticha-Ellis (1969) derived the exact solution for the double- and triple-beam cases. He also derived a second-order approximation for the many-beam case and a third-order approximation for the triple-beam case. However, even with a third-order approximation intensity calculations were limited to low secondary extinction and low absorption. Obviously, the exact solution can be applied in any situation of extinction and absorption. However, its limitation to a triple-beam case is a shortcoming. On the other hand, derivation of an exact solution for the many-beam case seems to be a formidable task owing to the multitude of cases concerning number and types of beams. The same can be said for the derivation of analytical formulas for higher-order approximations. In order to apply the



more convenient Moon and Shull's approximate solutions, Parente and Caticha-Ellis (1974a) derived a recurrence formula for the summation of the Taylor series expansion up to any desired order  $m$ . In the formulation presented by the authors the expansion, generalized for any beam  $i$ , can be written,

$$P_i(x) = P_i(0) + P_i^{(1)}(0)x + P_i^{(2)}(0)x^2/2! + \dots + P_i^{(m)}(0)x^m/m! + \dots \quad (1)$$

where the general term is given by:

$$(1/m!)x^m P_i^{(m)}(0) = (1/m!) \sum_k P_k(0) Y_{ki}^{(m)} \quad (2)$$

In the general term  $P_i^{(m)}(0)$  is the  $m$ th derivative of the power  $P_i(x)$  calculated at  $x=0$ , i.e.,

$$P_i^{(m)}(0) = d^m P_i(x) / dx^m \Big|_{x=0} .$$

$P_k(0)$  is the power of a beam  $k$  at the point  $x=0$  and the coefficient  $Y_{ki}^{(m)}$  is calculated from the coefficient of order  $(m-1)$  by

$$Y_{ij}^{(m)} = \sum_l X_{lj} Y_{il}^{(m-1)} . \quad (3)$$

where

$$X_{kj} = s_j \bar{Q}_{kj} x / \gamma_k \quad \text{for } k \neq j$$

and

$$X_{jj} = -s_j A_j x / \gamma_j \quad \text{for } k = j$$

The ratio  $x/\gamma_i = l_i$  corresponds to the effective path length of a beam  $i$  traversing a crystal layer of thickness  $x$  in an infinite crystal plate of thickness  $T$ . In general, the total power in beam  $i$  is required. In such a case,  $x$  is made equal to the plate thickness  $T$ .

Equation (3) is a recurrence formula that allows the calculation of the successive terms of the Taylor series expansion in an iterative way, i.e., the  $m$ th-order term is calculated as soon as the  $(m-1)$ th term is obtained. As implicit in the above formulation, the diffracted beams involved in the phenomenon can be of any type in any number. The coefficients for the first-order term ( $m=1$ ) are calculated from the coefficients of the zero-order term defined by

$$Y_{ki}^{(0)} = \begin{cases} 0 & \text{for } k \neq i \\ 1 & \text{for } k = i \end{cases} \quad (4)$$

The summation of the successive terms in (1), obtained by calculating iteratively the general term (2) to any desired order, gives the approximate intensity solution  $P_i(x)$  for beam  $i$ . Provided a computer is used, approximations with hundreds of terms can be calculated using the recurrence formula. It should be mentioned at this point that, even for a case involving high secondary extinction and/or high absorption, a good approximation can be attained, in general, with

a few tens of terms. An example is found in the work by Parente and Caticha-Ellis (1974b), where the 111 primary intensity of aluminum was measured with a single crystal in the shape of a square plate  $3\text{in} \times 3\text{in} \times 1\text{in}$  oriented with the (111) planes parallel to the  $3 \times 3$  face. Using the recurrence formula, the authors calculated intensities in four different interaction cases and compared them with experimental results. In spite of the quite high secondary extinction present in the measured intensities, a maximum of 14 terms revealed to be more than enough to obtain a good approximation in the four cases considered in the work.

Based on the theory outlined above, Parente, Mazzocchi and Pimentel (1994) derived intensity solutions appropriate for a many-beam case. Due to the employment of the recurrence formula in the derivation, the solutions are also appropriate to be used in cases involving high secondary extinction and/or high absorption. The approximate intensity solutions were derived by using the general term of the Taylor series expansion in the case of  $n$  beams diffracted in a crystal plate of thickness  $T$ .

Two solutions were derived, according to whether the beam  $i$  is reflected or transmitted,

$$R_i = - \left( \sum_{\substack{j=0 \\ j \neq i}}^{n-1} R_j C_{ji} \right) / C_{ii} \quad (5)$$

for a reflected beam, and

$$R_i = \sum_{\substack{j=0 \\ j \neq i}}^{n-1} R_j C_{ji} \dots \dots (6)$$

for a transmitted beam, where

$$R_i^r = P_i(T)/P_0(0)$$

$$R_i^t = P_i(0)/P_0(0)$$

$$\sum_m Y_{ji}^{(m)} / m! = C_{ji} \quad \text{for } j \neq i ,$$

and

$$1 + \sum_m Y_{ii}^{(m)} / m! = C_{ii} \quad \text{for } j = i .$$

In the above expressions, coefficients  $Y_{ji}^{(m)}$  and  $Y_{ji}^{(0)}$  are calculated by (3), in an iterative way, and  $P_0(0)$  is the power of the incident beam which is, of course, different from zero and, in general, not precisely known. Power ratios  $R_j$  corresponding to transmitted beams are null. Nevertheless, they contribute to the power of beam  $i$  through the coefficients  $C_{ji}$ ,  $C_{ii}$  included. It should be noted that, although the incident beam ( $j=0$ ) is always a transmitted beam,  $R_0 = 1$ . Because of this, the restriction  $j \neq i$  disappears if (6) is used to calculate

the intensity of the incident (transmitted) beam. Power ratios  $R_j$  corresponding to reflected beams can be determined from solution (5). A set of linear equations, with a maximum of  $n-2$  equations, is then obtained. The system of equations can be represented in a matrix form by (7)

$$\begin{pmatrix} C_{11} & C_{12} & \dots & C_{1n-1} \\ C_{21} & C_{22} & \dots & C_{2n-1} \\ \vdots & \vdots & \ddots & \vdots \\ C_{n-1,1} & C_{n-1,2} & \dots & C_{n-1,n-1} \end{pmatrix} \begin{pmatrix} R_1 \\ R_2 \\ \vdots \\ R_{n-1} \end{pmatrix} = - \begin{pmatrix} C_{n,1} \\ C_{n,2} \\ \vdots \\ C_{n,n-1} \end{pmatrix}$$

The system (7) can easily be solved if the number of equations is small. For a large number, one of several suitable subroutines available in computer libraries can be used. The approximate solution sought is obtained by substituting the  $R_j$ 's found by solving (7) in the appropriate equation, (5) or (6).

#### 4. MULTI - A Program for the Simulation of N.M.D. Patterns

In order to perform the structural analyses a computer program, MULTI, has been prepared aiming to calculate theoretical m.d. patterns (Mazzocchi, 1984; Parente, Mazzocchi and Pimentel, 1994). MULTI simulates point to point m.d. patterns for primary beams of any type and transmitted incident beams using the intensity solutions (5) or (6). A brief description of the main features of MULTI is given below:

1. For a predetermined primary reflection, it determines all possible secondary reflections occurring in a given interval of the azimuthal angle  $\phi$ . Primary reflection, angular interval of  $\phi$  and step  $\Delta\phi$  must be specified by the user.
2. It determines the characteristics of the beams, e.g. their signs  $s_i$  and their mean path lengths  $l_i$ .
3. For each  $\phi$ -position, it calculates the reflectivities for all interactions occurring in that position. A matrix of  $n(n-1)$  reflectivities is then obtained,  $n$  being the number of interacting beams.
4. As mentioned above, MULTI calculates the power of the beam, primary or incident, by using (5) or (6). When necessary, the system (7) formed to find the values of  $R_j \neq 0$  is solved by a subroutine adjoined to MULTI. The maximum order for the expansion is specified by the user.

#### 5. Structural Analysis of $\alpha$ - and $\beta$ -Quartz

$\alpha$ -quartz, one of the polymorphs of silica ( $\text{SiO}_2$ ) which is stable at room temperature, has a structure described by either of the two enantiomorphic trigonal space groups  $P3_121$  or  $P3_221$  (Wyckoff, 1965). At approximately 846K,  $\alpha$ -quartz undergoes a reversible transition to  $\beta$ -quartz with minor changes in the silicon and oxygen positions.  $\beta$ -quartz has a structure with hexagonal symmetry in either of the two enantiomorphic space groups  $P6_222$  or  $P6_122$  (Wyckoff, 1965). Both  $\alpha$ - and  $\beta$ -quartz have three molecules in hexagonal unit cells with almost the same dimension.  $\alpha$ - and  $\beta$ -quartz structures as described above correspond to well-known ordered models studied by several authors (see Wyckoff, 1965, for references). In a study dealing with the mechanism of the  $\alpha$ - $\beta$  phase transition in quartz, Young (1962) employing X-ray diffraction analysed the structures of both phases at high temperatures. The ordered model of structure suggested by Young for  $\beta$ -quartz is the same proposed by former authors where the silicon and oxygen atoms occupy, respectively, the special positions 3(c) and 6(j) in either of the above mentioned enantiomorphic hexagonal space groups (see Wyckoff, 1965). Wright and Lehmann (1981), employing high-resolution neutron diffraction data studied the  $\alpha$ - and  $\beta$ -quartz structures. These authors verified that for  $\beta$ -quartz the best agreement between the experimental intensity data and theoretical calculations is accomplished when a disordered structure is considered. In the structure of Wright and Lehmann, oxygen atoms occupy, in a half occupation mode, twice the number of special positions they occupy in the ordered model. Disordered positions are symmetrically placed around the 6(j) special positions in the ideal  $\beta$ -quartz structure.

The experimental measurements in quartz were carried out with a natural crystal shaped into an orthocylinder dimensioned 5cm $\times$ 5cm with the [001] crystallographic direction approximately parallel to the cylinder axis. Experimental primary and transmitted beams n.m.d. patterns, for both phases, were obtained with the crystal placed inside the furnace depicted in Figure 2. Well compacted vitreous silica powder maintained the crystal firmly in position inside the furnace. Measurements were done at room temperature, for  $\alpha$ -phase, and 1003 K, for the  $\beta$ -phase.

Analyses were done by calculating the integrated intensities of a few peaks, experimental and simulated, and comparing them by means of a R-factor given by

$$R = \frac{\sum_k |I_k(\text{obs}) - c \cdot I_k(\text{calc})|}{\sum_k I_k(\text{obs})} \quad (8)$$

where  $I_k(\text{obs})$  and  $I_k(\text{calc})$  are, respectively, observed and calculated integrated intensities of a peak  $k$ ;  $c$  is a scale factor which is varied in order to minimize  $R$ .

Table I shows the results found for  $\alpha$ -quartz and Table II for  $\beta$ -quartz. Values of  $R$  found in the analyses are indicated in the captions of the Tables.

## 6. Refinement of the Ferri- and Paramagnetic Phases of Magnetite

According to Verwey and co-workers (Verwey and de Boer, 1936; Verwey and Haayman, 1941; Verwey and Heilmann, 1947; Verwey, Haayman and Romeijn, 1947), above ca. 119 K, magnetite ( $\text{Fe}_3\text{O}_4$ ) is an inversed Fe spinel  $\text{Fe}^{3+}(\text{Fe}^{2+}\text{Fe}^{3+})\text{O}_4^{2-}$ . The inversed spinel structure of magnetite has a large unit cell containing 8  $\text{Fe}^{3+}$  ions in tetrahedral A sites and 8  $\text{Fe}^{2+}$  plus remaining 8  $\text{Fe}^{3+}$  ions in octahedral B

**Table I** - Results found for  $\alpha$ -quartz according the model proposed by Young (1962).  $R=0.344$

Azimuthal position of peaks		Integrated intensities	
$\phi$ (obs) (deg.)	$\phi$ (calc) (deg.)	$I_k(\text{obs})$	$I_k(\text{calc})$
61.29	61.23	2270.0	1623.4
61.90	61.98	1883.3	1004.8
2.69	62.69	2667.8	1237.2
63.76	63.80	251.5	263.8
64.75	64.82	1618.5	1777.2
69.44	69.05	5940.3	3890.5
71.22	71.27	5176.7	2047.3
71.86	-----	287.1	0
72.62	72.50	4666.2	7797.8
73.67	73.54	2704.6	4857.6
74.89	74.87	1139.9	1274.8
75.95	76.20	4207.4	4160.5
79.18	79.20	2413.8	2329.9
80.25	80.24	522.3	2486.9
82.30	82.20	10587.8	2876.2
83.70	83.76	1744.36	1375.3
84.32	84.36	1516.0	1139.8

sites. Ions in magnetite are distributed in the following positions of space group  $\text{Fd}\bar{3}\text{m}$ :  $\text{O}^{2-}$  in 32(e),  $\text{Fe}^{2+}$  and  $\text{Fe}^{3+}$  in equal numbers and random distribution in 16(d) and  $\text{Fe}^{3+}$  in 8(a).

The magnetic structure of magnetite, at room temperature, is type Néel A-B. Néel (1948) accounting for the observed magnitude of the saturation magnetic moment, which could only result from the ferrous ions alone, postulated that the ions on the A sites in magnetite were coupled antiferromagnetically to those on the B sites. In such a coupling, in fact, the contribution of the ferric ions is null since they are distributed in equal numbers on both A and B sites. On the other hand, the contribution of the ferrous ions is maximum, since all

**Table II** - Results found in the analyses of  $\beta$ -quartz for the ordered (Young, 1962) and disordered model (Wright and Lehmann, 1981).  $R=0.143$  and  $R=0.110$ , respectively.

Observed		Calculated for the ordered model		Calculated for the disordered model	
$\phi$ (obs) (deg.)	$I_k(\text{obs})$	$\phi$ (calc) (deg.)	$I_k(\text{calc})$	$\phi$ (calc) (deg.)	$I_k(\text{calc})$
50.34	957.4	50.63	825.1	50.36	871.35
59.04	912.3	59.12	1136.2	59.13	962.93
60.90	1166.0	60.87	1103.8	60.87	943.50
69.57	809.3	69.65	164.2	69.64	832.50
84.68	246.8	84.77	416.9	84.77	274.73
88.59	405.8	88.62	848.9	88.63	419.03
91.29	344.0	91.37	432.0	91.37	452.33
95.22	256.5	95.23	181.4	95.23	321.90
103.42	439.3	103.40	378.0	103.41	505.05
104.51	585.8	104.58	794.9	104.59	740.93
110.30	1013.0	110.35	794.9	110.36	860.25
119.02	1069.1	118.85	1131.8	118.90	957.38
120.83	1006.7	120.87	1164.2	120.87	993.45
129.61	826.6	129.65	803.5	129.65	826.95

of them are on the B sites. This configures a ferrimagnetic structure. Above the Curie temperature, ca. 853 K, magnetite is magnetically disordered, i.e. it is a paramagnet.

The experimental measurements were carried out with a natural magnetite single crystal. The crystal was placed firmly inside the furnace depicted in Figure 2. For this work, both resistance and sustaining powder were substituted by more appropriate materials (Mazzocchi and Parente, 1997). The crystal was fixed in the center of the furnace with the previously oriented  $\langle 111 \rangle$  direction nearly parallel to the  $\phi$ -axis. Multiple diffraction data were taken at room temperature and 976 K. We assumed that, at this temperature, the crystal was wholly in the paramagnetic phase.

The  $\phi$ -scans were carried out in steps of  $0.1^\circ$ , 5 min of counting time each step, over an azimuthal angular interval extending from  $0$  to  $83.5^\circ$  for both patterns. Complete  $60^\circ$  patterns were obtained in this interval, which is in accordance with the existence of 3-fold symmetry axes along the  $[111]$  directions in the cubic system (Chang, 1984). Since half of a  $60^\circ$  pattern is a mirrored image of the other half (Mazzocchi and Parente, 1994), the halves were summed to form a  $30^\circ$  pattern with double intensity.

A process based on the parameter-shift method (Buihaya and Stanley, 1963) was employed in the refinements of the structural parameters (Mazzocchi and Parente, 1997).

The  $R$  factor used is similar to the profile  $R$  factor of Rietveld (1969), used by him to evaluate the agreement between profiles. It is given by the same formula (8) used for the study of  $\alpha$ - and  $\beta$ -quartz.

However, now  $I_k(\text{obs})$  and  $I_k(\text{calc})$  are, respectively, observed and calculated intensities in a  $k^{\text{th}}$  azimuthal position;  $c$  is a scale factor which is varied in order to minimize  $R$ , during a cycle of refinement, for each value assumed for a certain parameter in its interval of variation. The refinements were done in a point-to-point basis, i.e. for each  $I_k(\text{obs})$  a corresponding  $I_k(\text{calc})$  was calculated by MULTI using a given set of structural parameters (Mazzocchi and Parente, 1997).

In a first refinement (I), an overall isotropic thermal parameter  $B$  was assumed for all ions in the structure. In a second refinement (II), different isotropic parameters were assumed for the special positions in the space group. They are identified by  $B_a$ ,  $B_d$  and  $B_e$  for the positions 8(a), 16(d) and 32(e), respectively. Finally, anisotropic thermal parameters were assumed in a third refinement (III). In refinements I and II, the standard deviation of the gaussian distribution ( $\eta$ ), assumed in the simulations by MULTI, were maintained constant. In refinements III,  $\eta$  was refined together with the structural parameters.

Refinements I, II and III, for the ferrimagnetic phase, were done in accordance with the process outlined above. Results of such refinements are listed in Table III. In Figure 3, the experimental n.m.d. pattern of the ferrimagnetic phase is compared to simulated patterns calculated by MULTI with the final sets of parameters found in the refinements I, II and III. Figure 3 also

**Table III** - Lattice, positional and thermal parameters found in the refinements of the ferrimagnetic phase of magnetite.

POSITIONS	PARAM-ETERS	REFIN. I	REFIN. II	REFIN. III
8(a)	a ( $\text{\AA}$ )	8.401(0)	8.402(0)	8.399(6)
	B ( $\text{\AA}^2$ )	1.15(0)	-	-
	$B_a$ ( $\text{\AA}^2$ )	-	0.90(0)	-
	$B_{11}$ ( $\text{\AA}^2$ )	-	-	0.28(0)
16(d)	$B_d$ ( $\text{\AA}^2$ )	-	1.1(3)	-
	$B_{11}$ ( $\text{\AA}^2$ )	-	-	0.63(5)
	$B_{12}$ ( $\text{\AA}^2$ )	-	-	0.27(5)
32(e)	x	0.370(5)	0.370(0)	0.370(7)
	$B_e$ ( $\text{\AA}^2$ )	-	1.3(0)	-
	$B_{11}$ ( $\text{\AA}^2$ )	-	-	0.07(7)
	$B_{12}$ ( $\text{\AA}^2$ )	-	-	0.00(8)
	$\eta$ (rad)	-	-	0.0062(6)
	C ( $\times 10^5$ )	1.620	1.630	2.285
	R (%)	3.99	3.96	3.00

shows the corresponding difference patterns obtained by calculating  $w_k [I_k(\text{obs}) - c \cdot I_k(\text{calc})]$ , where the weighting factor is given by  $w_k = I_k(\text{obs})^{-1/2}$ . A

**Table IV** - Lattice, positional and thermal parameters found in the refinements of the paramagnetic phase of magnetite.

POSITIONS	PARAM-ETERS	REFIN. I	REFIN. II	REFIN. III
8(a)	a ( $\text{\AA}$ )	8.486(0)	8.490(5)	8.491(3)
	B ( $\text{\AA}^2$ )	1.42(5)	-	-
	$B_a$ ( $\text{\AA}^2$ )	-	1.8(5)	-
	$B_{11}$ ( $\text{\AA}^2$ )	-	-	0.26(0)
16(d)	$B_d$ ( $\text{\AA}^2$ )	-	1.1(5)	-
	$B_{11}$ ( $\text{\AA}^2$ )	-	-	0.41(0)
	$B_{12}$ ( $\text{\AA}^2$ )	-	-	-0.00(9)
32(e)	x	0.381(5)	0.381(5)	0.381(7)
	$B_e$ ( $\text{\AA}^2$ )	-	1.8(0)	-
	$B_{11}$ ( $\text{\AA}^2$ )	-	-	0.19(8)
	$B_{12}$ ( $\text{\AA}^2$ )	-	-	0.18(3)
	$\eta$ (rad)	-	-	0.0051(2)
	C ( $\times 10^5$ )	2.040	1.995	2.380
	R (%)	3.56	3.46	3.32

qualitative evaluation of the comparisons shows that refinement III clearly exhibits the best agreement whereas the differences between refinements I and II are almost negligible. Values of  $R$  in Table III confirm above assertions.

Figure 4 is the equivalent of Figure 3 for the paramagnetic phase. Differently from Figure 3, a comparison between refinements I, II and III shows no remarkable differences. In fact, the values of  $R$  listed in Table IV are very little different although diminishing from refinement I thru III.

## 7. Commentaries

Observing the results of the applications of n.m.d. as a method for structural analysis, reported in this work, one can say, at least, they are 'normal' results when compared to those obtained in a standard method.

This is particularly true for the refinement done in the n.m.d. data obtained for the magnetic phases of magnetite. As a matter of fact, simulated and experimental patterns, in this case, agreed within a few percent as commonly occurs when applying a standard method. On the other hand, the results for quartz are not good. It is important to note, however, in the quartz analysis no refinement of structural parameters has been tried. Of course, many questions can be posed concerning many aspects of the n.m.d. method. But, it must be said this is a quite new method demanding further investigations. Nevertheless, a few observations about it are done below, taking into account the 'state-of-the-art' of multiple diffraction and its applications.



- It is a single-crystal method and, as such, intensities are affected by extinction. In n.m.d., secondary extinction is particularly important. However, theory used intrinsically corrects for this effect.
- Multiple diffraction is a disturbing phenomenon in standard single-crystal diffractometry. In n.m.d., on the other hand, clearly multiple diffraction causes no disturbing effects since it is the essence of the method, at all.
- Data acquisition in single-crystal diffractometry demands a rather complicated procedure involving spatial orientation of crystal and positioning ( $2\theta$ ) of detector, for each observed reflection. In n.m.d., except for the  $\phi$ -scan, experiment is performed in a 'steady state', i.e. crystal and detector are positioned once.
- In single crystal diffractometry intensities are, in general, univocally correlated to the square of the structure factors of reflections. In n.m.d., in the simplest case (three-beam diffraction) there are six correlations to be considered. In a general case,  $n(n-1)$  correlations must be considered.

Except for the last commentary above, all others are, no doubt, 'pros' rather than 'cons'. Certainly many 'cons' will be found with further investigations about n.m.d. (and x.m.d., X-ray multiple diffraction, as well). Perhaps, in the future, one could say 'In this single crystal too much extinction and multiple diffraction occur. Why not try the n.m.d. method?'

#### Acknowledgments

The authors acknowledge the support given by Conselho Nacional de Desenvolvimento Científico e Tecnológico (CNPq), under contracts nos. 400397/93-5 and 300136/94-3 (RE), as well as International Atomic Energy Agency (IAEA), under research contract no. 6974/R2/RB.

#### References

- [1] U.W. Arndt and B.T.M. Willis, *Single crystal diffractometry*, Cambridge University Press, 1966.
- [2] G.E. Bacon, L.D. Lowde, *Acta Cryst.* **1** (1948) 303-314.
- [3] G. Borgonovi, G. Caglioti, *Nuovo Cim.* **24** (1962) 1174.
- [4] A.K. Buiya, E. Stanley, *Acta Cryst.* **16** (1963) 981-984.
- [5] S. Caticha-Ellis, *Acta Cryst. A* **25** (1969) 666-673.
- [6] S.-L. Chang, *Appl. Phys. A* **26** (1981) 221.
- [7] S.-L. Chang, *Phys. Rev. Lett.* **48** (1982) 163.
- [8] S.-L. Chang, *Multiple diffraction of X-ray in crystals*, Berlin/Heidelberg/New York/Tokyo: Springer-Verlag, 1984.
- [9] H. Cole, F.W. Chambers, H.M. Dunn, *Acta Cryst.* **15** (1962) 138-144.

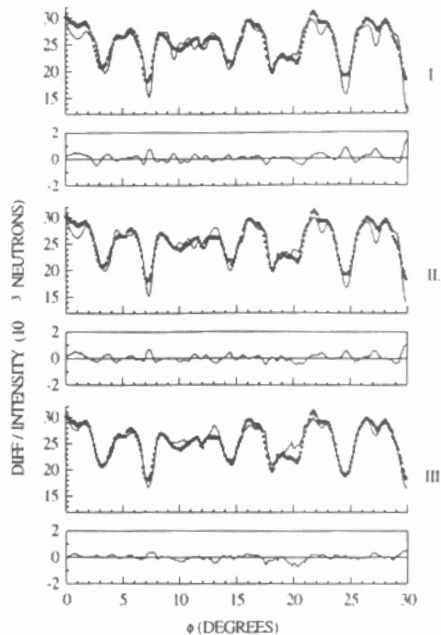


**Fig.3** Comparisons between the experimental n.m.d. pattern obtained for the ferrimagnetic phase of magnetite and simulated patterns after refinements I, II and III.

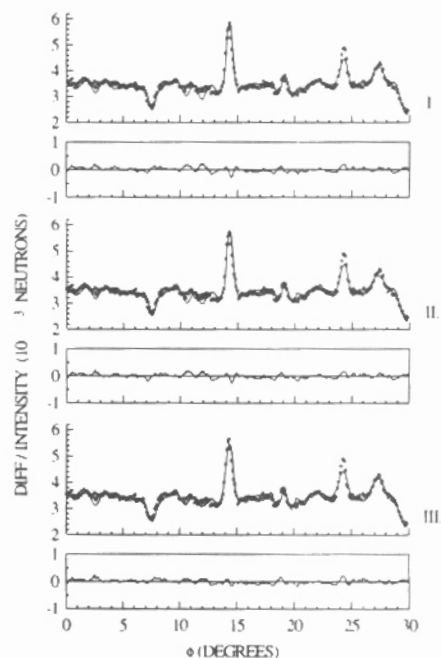


**Fig. 4** Comparisons between the experimental n.m.d. pattern obtained for the paramagnetic phase of magnetite and simulated patterns after refinements I, II and III.



- [10] C. Giacobozzo, H.L. Monaco, D. Viterbo, F. Scordari, G. Gilli, M. Zanotti, M. Catti, *Fundamentals of crystallography*. IUCr Texts on Crystallography-2, Oxford University Press Inc., New York, 1994.
- [11] V.L. Mazzocchi, *Estudo das fases  $\alpha$  e  $\beta$  do quartzo com difração múltipla de nêutrons*. Master's thesis, Univ. de São Paulo, Brazil, 1984.
- [12] V.L. Mazzocchi, C.B.R. Parente, *J. Appl. Cryst.* **27** (1994) 475-481.
- [13] V.L. Mazzocchi, C.B.R. Parente, Submitted to *Journal of Applied Crystallography* (1997).
- [14] R.M. Moon, C.G. Shull, *Acta Cryst.* **17** (1964) 805-812.
- [15] L. Néel, *Ann. Physique* **3** (1948) 137-198.
- [16] C.B.R. Parente, S. Caticha-Ellis, *Japan. J. Appl. Phys.* **13** (1974a) 10, 1501-1505.
- [17] C.B.R. Parente, S. Caticha-Ellis, *Japan. J. Appl. Phys.* **13** (1974b) 10, 1506-1513.
- [18] C.B.R. Parente, V.L. Mazzocchi, F.J.F. Pimentel, *J. Appl. Cryst.* **27** (1994) 463-474.
- [19] B. Post, *Rev. Lett.* **39** (1977) 760.
- [20] B. Post, *Acta Cryst. A* **35** (1979) 17.
- [21] M. Renninger, *Z. Phys.* **106** (1937) 141-176.
- [22] H.M. Rietveld, *J. Appl. Cryst.* **2** (1969) 65-71.
- [23] E.J.W. Verwey, J.H. de Boer, *Rec. Trav. Chim.* **55** (1936) 531-540.
- [24] E.J.W. Verwey, P.W. Haayman, *Physica VIII* **9** (1941) 979-987.
- [25] E.J.W. Verwey, P.W. Haayman, F.C. Romeijn, *J. Chem. Phys.* **15** (1947) 4, 181-187.
- [26] E.J.W. Verwey, E.L. Heilmann, *J. Chem. Phys.* **15** (1947) 4, 174-180.
- [27] A.F. Wright, M.S. Lehmann, *J. Solid State Chem.* **36** (1981) 371-380.
- [28] R.W.G. Wyckoff, *Crystal Structure*, 2<sup>nd</sup> Ed., Vol.1. New York, Wiley, 1965
- [29] R.A. Young, *Mechanism of the phase transition in quartz*, Final Report, Contract no. AF 49 (683)-624. Project A-447. ASTIA. Catalog no. 276235. Georgia Institute of Technology, Atlanta, Georgia, USA (1962).